C. B. McKee, S. Steiger, G. Crater, *Nucleic Acids Res.* **15**, 10031 (1987); J. Noolandi, G. W. Slater, H. A. Lim, J. L. Viovy, *Science* **243**, 1456 (1989); J. Stellwagen and N. C. Stellwagen, *Nucleic Acids Res.* **17**, 1537 (1989); D. C. Schwartz and M. Koval, *Nature* **338**, 520 (1989); S. B. Smith, P. K. Aldridge, J. B. Callis, *Science* **243**, 203 (1989); S. Gurrieri, E. Rizzarelli, D. Beach, C. Bustamante, *Biochemistry* **29**, 3401 (1990); B. H. Zimm, *J. Chem. Phys.* **94**, 2187 (1991); E. D. T. Atkins and M. A. Taylor, *Biopolymers* **32**, 911 (1992).

9. We scored cutting frequencies by counting cuts in molecules present in microscope fields (containing typically three to five molecules). About half of the fields showed no cutting and were not scored, resulting in an underestimate of the number of uncut molecules. The cutting frequency results for chromosome 5 digested with Not I show that the number of fully cut molecules is approximately half that of all singly cut molecules: we calculate the value corresponding to complete digestion by assuming that an equal distribution of identically sized chromosome 5 and 8 DNA molecules are present in the mounted sample. The Not I restriction maps for these chromosomes reveal that chromosome 5 has three cut sites, whereas chromosome 8 has only two. Chromosome 11 cutting frequency data are different: 25% of all cut molecules are seen to be fully digested (two cutting sites). An explanation for the apparently lower frequency is that this chromosome produces a 30-kb-sized Not I fragment that is more difficult to detect optically than larger fragments. Observation of 1000-kb-sized molecules such as chromosome 13 and 16 shows that roughly half of the molecules are digested to completion (one cut) in mounts with scorable cutting activity.
10. A. J. Link and M. V. Olson, *Genetics* **127**, 681 (1991).
11. Absolute intensities from individual images (Not I fragments from chromosomes 1 and 11) were calculated (*6*) and plotted against change of apparent length over a time interval typically used in optical mapping (10 to 15 min). Data from images with poor focus were discarded. For each sample, we calculated the initial intensity by averaging absolute intensity values from groups of five adjacent images and taking the largest value. We normalized the values from several samples by dividing values from each image by the initial intensity for the sample.
12. A collection of genetically mapped Southern (DNA) hybridization probes were used to create ordered PFGE restriction maps for comparison with optical mapping results: Chromosome 3 (*LEU2, MAT*), chromosome 9 (*THS1, SEC11, SUC2, CAP2*), chromosome 11 (*SIR1, MAK11, URA1, APE2*). Relative apparent length results are given assuming random sampling from a normal population. When the number of samples is less than six, the pooled SD from the Not I results is used to calculate the confidence interval. Chromosome enzyme (our PFGE size/total size), mean ± 90% confidence kb/population SD ± 90% confidence kb (number of samples): 3 Rsr II (250/350) 264 ± 31/58 ± 25 (8), 3 Rsr II (95/350) 86 ± 31/58 ± 25 (8); 11 Csp I (292/675) 288 ± 30/72 ± 23 (14), 11 Csp I (143/675) 193 ± 43/101 ± 32 (14), 11 Csp I (240/675) 194 ± 27/65 ± 21 (14); 9 Csp I (145.5/455) 138 ± 35/47 (5), 9 Csp I (20/455) 17 ± 35/47 (5), 9 Csp I (82/455) 151 ± 35/47 (5), 9 Csp I (194/455) 149 ± 35/47 (5). Relative fluorescence intensity results after two dilations of backbone, assuming random sampling from a normal population. Chromosome enzyme (our PFGE size/total size), mean ± 90% confidence kb/population SD ± 90% confidence kb (number of samples): 3 Rsr II (250/350) 256 ± 20/37 ± 16 (8), 3 Rsr II (95/350) 94 ± 20/37 ± 16 (8); 11 Csp I (292/675) 279 ± 24/45 ± 20 (8), 11 Csp I (143/675) 204 ± 33/61 ± 27 (8), 11 Csp I (240/675) 191 ± 20/38 ± 17 (8); 9 Csp I (145.5/455) 128 ± 34/36 (3), 9 Csp I (20/455) 14 ± 34/36 (3), 9 Csp I (82/455) 150 ± 34/36 (3), 9 Csp I (194/455) 163 ± 34/36 (3).
13. L. L. Cavalli-Sforza, *Am. J. Hum. Genet.* **46**, 649 (1990).
14. We thank I. Maity and M. Hsu for technical assistance, N. Kallenbach for helpful suggestions, and N. Seeman and his laboratory for synthesis of oligonucleotides. Supported by grants from the NIH (HG00225-01), the NSF, the W. M. Keck Foundation, and the Lucille P. Markey Charitable Trust. D.C.S. is a Lucille P. Markey Scholar.

19 February 1993; accepted 10 June 1993

Erythrocyte P Antigen: Cellular Receptor for B19 Parvovirus

Kevin E. Brown,* Stacie M. Anderson, Neal S. Young

The pathogenic human parvovirus B19 replicates only in erythroid progenitor cells. This virus was shown to bind to blood-group P antigen, as measured by hemagglutination. Erythrocytes lacking P antigen were not agglutinated with B19. Purified P antigen (globoside) blocked the binding of the virus to erythroid cells and the infectivity of the virus in a hematopoietic colony assay. Target cells were protected from infection by preincubation with monoclonal antibody to globoside. Knowledge of a parvovirus receptor has implications for understanding the pathogenesis of parvovirus infections and for the use of parvoviruses in gene therapy.

The only known pathogenic human parvovirus, B19 parvovirus, causes the common illness fifth disease in normal individuals (*1*), transient aplastic crisis in patients with underlying hemolysis (*2*), and chronic anemia from persistent infection in immunocompromised patients (*3*). Parvovirus infection in pregnancy can lead to hydrops fetalis and fetal loss (*4*) or congenital infection (*5*). In contrast to most viruses, B19 parvovirus is tropic for one highly differentiated cell type, the human erythroid progenitor, and tropism might be mediated by a cellular receptor unique to cells of the erythroid lineage. Cellular receptors are known for influenza A, rabies, human immunodeficiency and Epstein-Barr viruses, as well as several of the picornaviruses (*6*), but none has been described for any of the *Parvoviridae*.

Most parvoviruses can agglutinate erythrocytes, and the results of early attempts to remove the hemagglutinin of rodent parvoviruses from guinea pig erythrocytes by chemical methods or neuraminidase suggested that binding might be mediated by a glycolipid (*7*). Enzymatic treatment of target cells in binding assays implicated sialic acid in the context of a glycoprotein for the hemagglutination of feline panleukopenia virus (*8*) and the cellular binding of minute virus of mice, a rodent parvovirus (*9*). These results all suggest the importance of carbohydrate antigens for parvovirus binding. However, the precise nature of the receptor is not known for any of these viruses.

We have shown that B19 parvovirus empty capsids (*10*) agglutinated human red cells (*11*), and we tested the ability of membrane extracts from different cell types to block B19 binding. Membrane extracts were prepared by means of 10 mM CHAPS to solubilize proteins and lipids. Extracts from human erythrocyte ghosts (*12*) or cells permissive for B19 parvovirus [human bone marrow and UT-7 leukemic cells (*13*)] blocked hemagglutination. In contrast, extracts from K562, HL-60, and HeLa cells, which are not permissive for the virus, did not block binding.

Trypsin (0.2%; 1 hour at 37°C) and neuraminidase (0.1 U ml^{-1}; 1 hour at 37°C) each increased binding (a 4 log_2 and a 3 log_2 increase in hemagglutination (HA) titer, respectively), suggesting that protein and sialic acid were not involved and that modification of the red cell membrane by these agents might expose binding sites. Treatment with sodium periodate (10 mM; 15 min at 37°C) markedly reduced the binding of virus to erythrocytes [>4 log_2 decrease in HA titer (5 μM sodium periodate treatment overnight did not reduce binding)], implicating carbohydrates other than sialic acid. Phosphoinositol-specific phospholipase C and reducing agents did not affect binding.

Human erythrocyte ghosts (*12*) were then treated with CHAPS, the solubilized extract was incubated with agarose-immobilized enzymes overnight at 37°C, and the supernatant was tested in the hemagglutination inhibition assay (*11*). Pretreatment of red cell extract with immobilized phospholipase A_2 removed activity completely, whereas treatment with immobilized proteases had no significant effect. These results suggest that the inhibitor was either a lipid or that a lipid was important in maintaining

Hematology Branch, National Heart, Lung and Blood Institute, Bethesda, MD 20892.

*To whom correspondence should be addressed.

a correct conformation. In addition, the hemagglutination inhibitor also partitioned into the organic phase of a water-butanol mixture and into the lower, or lipid, phase of a chloroform-methanol–salt solution mixture (*14*).

Confirmation that inhibitor activity was in the lipid fraction was obtained by the preparation of a pure lipid extract (*15*), followed by fractionation by either silica gel column or DEAE-cellulose acetate (*16*). Inhibitor activity eluted with methanol or 1:1 chloroform:methanol, consistent with the properties of a ceramide oligohexoside (Table 1). A mixture of purified ceramide oligohexosides strongly inhibited hemagglutination by the virus. Assays of individual glycolipids showed that the inhibitory activity was maximal for a ceramide (Cer) tetrahexoside, globotetraosylceramide [or globoside, *N*-acetylgalactosamine (GalNAc)(β1–3)Gal(α1–4)Gal(β1–4)GlcCer; Gal, galactose; Glc, glucose)] (Table 2).

Globoside is a member of the P blood-group system, which contains two common antigens, P_1 and P, and the much rarer P^k antigen (*17*). The P^k antigen [ceramide trihexoside (CTH) globotriaosylceramide: Gal(α1–4)Gal(β1–4)GlcCer] is a normal precursor of P. The P_1 antigen is an unrelated lactoneotetraose ceramide derivative. Red cells of individuals with blood-group P_1 phenotype have P_1 and P antigens; individuals with P_1^k phenotype have P_1 and P^k antigens; individuals with P_1 phenotype have P antigen alone; and individuals with the rare p phenotype lack all three antigens. Forssman antigen is not a normal constituent of human cells but a pentahexoside containing the same saccharide sequence as globoside with the addition of a terminal *N*-acetylgalactosamine residue.

Red cells from 26 individuals with different phenotypes of the blood-group P system were tested for their ability to agglutinate with parvovirus B19 (Fig. 1). Only cells containing P antigen hemagglutinated: P_1 phenotype (geometric) mean HA titer was 40,000 (n = 11); P_2 phenotype (geometric) mean HA titer was 32,000 (n = 6); and P_1^k and p phenotypes were <200 (n = 1 and 8, respectively).

The binding of viral capsids to globoside was demonstrated by thin-layer chromatography, in which a mouse anti-B19–specific monoclonal antibody and a second anti-

Table 1. Hemagglutination inhibition (HAI) titers of red cell lipids fractionated on different columns. Lipids were extracted from red cell ghosts (*12, 15*) and fractionated on either a silica gel or a DEAE-cellulose–acetate column (*16*). Organic solvents were removed by evaporation, and salts were removed by dialysis against water and lyophilization. The residual pellets were resuspended in saline and tested in the hemagglutination assay.

Eluant	Lipids eluted	HAI titer
	Silica gel column	
Chloroform	simple lipids	<10
Acetone	glycolipids	<10
Methanol	ceramide oligohexosides and polar lipids	2560
	DEAE-cellulose–acetate column	
Chloroform	simple lipids	80
Chloroform:methanol (9:1)	ceramide monohexoside phosphatidylcholine	640
Chloroform:methanol (1:1)	ceramide oligohexoside phosphatidyl-ethanolamine	1280
Methanol		<10
Acetic acid	phosphatidylserine	<10
Ammonium acetate	phosphatidylinositol phospatidylglycerol	<10

Table 2. Hemagglutination inhibition titers of purified glycosphingolipids. Purified glycosphingolipids [Sigma or BioCarb (Lund, Sweden)] were dissolved in saline (1 mg ml^{-1}) and tested by HAI assay (*11*). Abbreviations: Fuc, fucose; GlcNAc, *N*-acetylglucosamine.

Purified glycosphingolipid	Structure	HAI titer
Lactosyl ceramide	Gal(β1–4)GlcCer	<10
CTH, P^k	Gal(α1–4)Gal(β1–4)GlcCer	<10
Globoside, P	GalNAc(β1–3)Gal(α1–4)Gal(β1–4)GlcCer	25600
Forssman	GalNAc(α1–3)GalNAc(β1–3)Gal(α1–4)Gal(β1–4)GlcCer	200
Asialoganglioside GM2	GalNAc(β1–4)Gal(β1–4)GlcCer	<10
Lacto-*N*-fucopentaose (LNF1)	Fuc(α1–2)Gal(β1–3)GlcNAc(β1–3)Gal(β1–4)GlcCer	<10

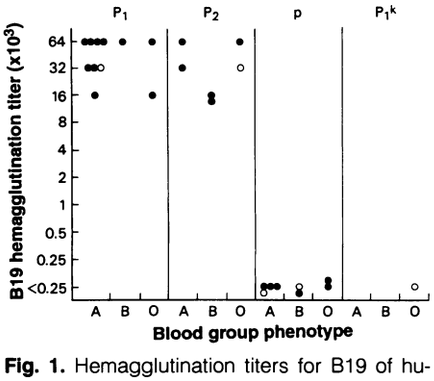

Fig. 1. Hemagglutination titers for B19 of human erythrocytes with different P phenotypes. Erythrocytes were washed, suspended in saline (0.5% v/v), and assayed with the use of recombinant B19 capsids (1 mg ml^{-1}) (*11*). Filled circles, rhesus-positive cells; open circles, rhesus-negative cells.

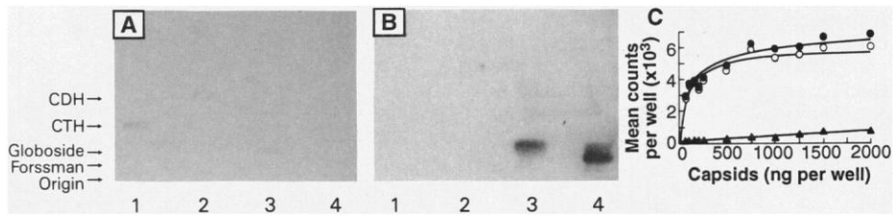

Fig. 2. The binding of B19 parvovirus empty capsids (*10*) to purified neutral lipids. Each purified glycosphingolipid (5 μg; Sigma or BioCarb) was applied to a silica plate (ICN Biochemicals, Costa Mesa, CA) and analyzed by thin-layer chromatography with chloroform:methanol:water (65:25:4). (**A**) The plates were exposed to I_2 vapor, and the position of the bands was marked. (**B**) Nonspecific binding was blocked with 0.1% poly isobutyl methacrylate in hexane (1 min) and 3% bovine albumin in phosphate-buffered saline (2 hours) before the plates were sequentially incubated with B19 empty capsids. Binding was then blocked by mouse anti-B19 monoclonal antibody (Chemicon) followed by ^{125}I-labeled sheep anti-mouse antibody (Amersham). The plates were dried and exposed to x-ray film overnight. Lanes: 1, CDH; 2, CTH; 3, globoside; 4, Forssman antigen. No bands were visible when diluent was substituted for empty capsids. (**C**) Binding-affinity curve derived from different concentrations of globoside in the radioimmunoassay (*18*). Filled triangles, nonspecific binding; filled circles, total binding to globoside; open circles, specific binding to globoside.

mouse antibody were used for the detection of the bound virus. The capsids showed strong binding to purified globoside and Forssman antigens (Fig. 2, A and B). In a radioimmunoassay, binding (*18*) was specific and showed saturability, with 50% occupancy at 100 ng per well (that is, 3×10^{-10} M) (Fig. 2C) (*19*).

Parvovirus B19 is highly toxic to the production of erythroid colonies from late erythroid colony-forming units (CFU-E) in methylcellulose culture (*20*), the system that was used as an assay for B19 infection. Colony formation from CFU-E was protected from the cytopathic effect of B19 parvovirus in the presence of globoside, consistent with the inhibition of viral infection by a soluble receptor (Fig. 3A). Forssman antigen was also protective, but there was no effect by CTH, ceramide dihexoside (CDH), or lactosylceramide. Protection of erythroid colony formation was dependent on the dose of globoside (Fig. 3B). These results suggested that P antigen competed with the putative binding site on target cells for the virus.

To show that P antigen was the major receptor for parvovirus B19 on erythroid target cells, monoclonal antibodies to blood-group P antigens were used to prevent viral binding. Parvovirus cytotoxicity for CFU-E was abrogated by the pretreatment of target cells with monoclonal antibody to globoside (*21*) (Fig. 4). There was no protection with similar concentrations of monoclonal antibodies against P_1 or P^k. (In other experiments with monoclonal ascites to globoside, cytotoxicity could be completely inhibited.)

Our findings show that B19 capsids bind to P antigen and that B19 infection can be blocked by excess globoside or by a globoside-specific monoclonal antibody (*22*). These results indicate that P antigen is a B19 virus receptor. The tetrasaccharide chain appears to mediate binding specifically, because ceramides with other saccharide chains do not have this effect and B19 capsids also bind to immobilized globotetraose (the tetrasaccharide of globoside). The free tetrasaccharide chain alone did not appear to block binding, and the ceramide may be important to the maintenance of the carbohydrate moiety in the proper structural conformation.

The tissue distribution of P is consistent and helps explain the extreme tropism of B19 parvovirus for erythroid cells. However, viral replication may also be modulated by specific erythroid transcription factors (*23*). The presence of P on cells not known to be permissive for viral replication has pathophysiologic implications. Endothelial cells (*21*) may be the targets of viral infection that mediate transplacental transmission and contribute to the rash of fifth disease. The P antigen is also found on fetal cardiac myocytes (*24*), consistent with evidence that the fetus infected with B19 can develop myocarditis (*25*). Parvovirus is now implicated in paroxysmal cold hemoglobinura, a severe hemolytic anemia characterized by the Donath-Landsteiner antibody of anti-P specificity (*26*), either by the development of anti-idiotypic antibodies or by the recognition of the virus-receptor complex as a neoantigen. Finally, the lipid character of the cell membrane is amenable to chemical modification; if a functional globoside receptor can be introduced, such a method could be used in gene therapy strategies that are based on parvoviruses (*27*).

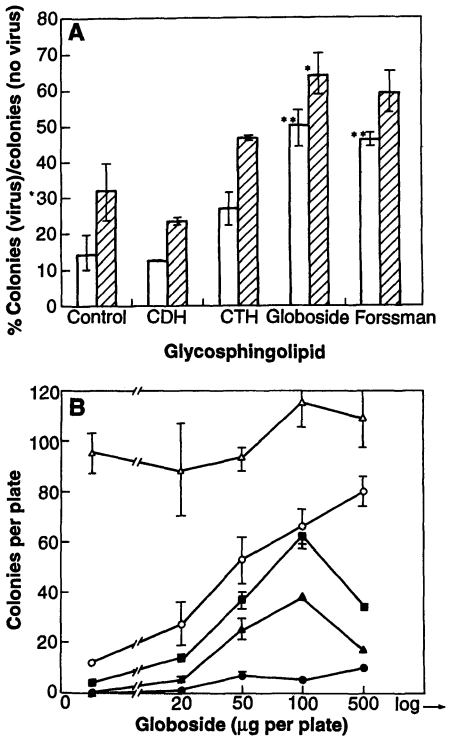

Fig. 3. Inhibition of B19 parvovirus infection with globoside. The B19 parvovirus was preincubated with (**A**) different purified glycosphingolipids [100 μg per plate (Sigma or BioCarb)] and (**B**) different globoside concentrations for 2 hours and then mixed with bone-marrow mononuclear cells for 2 more hours. The cell mixtures were cultured in methylcellulose (*20*), and CFU-E were assayed by the microscopic examination of the plates 7 days later. The results in (A) are plotted as a ratio of the mean number of colonies on the plates with no virus added (201 CFU-E per 10^5 bone-marrow mononuclear cells was equivalent to 100%). In (A), open bars indicate 50×10^9 and hatched bars 20×10^9 B19 virus particles per plate. (A) and (B) were performed with bone marrow from different donors; experimental variability is likely contributed to by marked variation among normal individuals in colony-forming ability in tissue culture, the insolubility of glycolipids, and the level of contamination of marrow preparations with erythrocytes bearing globoside. Bars indicate SEM. Asterisk, $P < 0.01$; two asterisks, $P < 0.001$, compared to control colony numbers. In (B), open triangles represent 0, open circles 5×10^9, filled squares 10×10^9, filled triangles 20×10^9, and filled circles 50×10^9 B19 virus particles per plate.

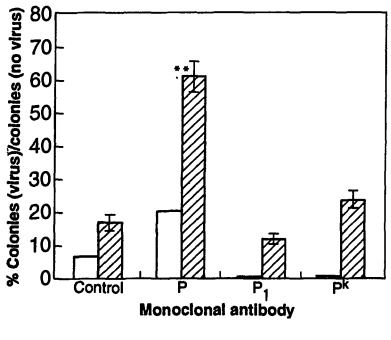

Fig. 4. Inhibition of B19 infection with monoclonal antibody to P antigen. Mouse monoclonal antibodies to P antigen (*21*), P_1, or P^k (BioCarb) were diluted (2 μg ml^{-1}) and incubated with bone-marrow mononuclear cells for 2 hours. Purified B19 parvovirus was added for 2 more hours before the cell mixtures were cultured in methylcellulose (*20*), and CFU-E were assayed 7 days later. The results are plotted as a ratio of the mean number of colonies on the plates with no virus added (29.5 CFU-E per 10^5 bone-marrow mononuclear cells was equivalent to 100%). Bars indicate SEM. Two asterisks, $P < 0.001$, compared to control colony numbers. Open bars, 50×10^9; and hatched bars, 20×10^9 B19 particles per plate.

REFERENCES AND NOTES

1. M. J. Anderson *et al.*, *Lancet* i, 1378 (1983).
2. N. Young, *Semin. Hematol.* **25**, 159 (1988).
3. N. Frickhofen *et al.*, *Ann. Intern. Med.* **113**, 926 (1990).
4. K. E. Brown, *Br. J. Obstet. Gynaecol.* **96**, 764 (1989).
5. ———, J. Antunez-de-Mayolo, N. S. Young, unpublished results.
6. T. L. Lentz, *J. Gen. Virol.* **71**, 751 (1990).
7. G. Cocuzza and G. Russo, *Boll. Ist. Sieroter. Milan.* **48**, 204 (1969).
8. M. Mochizuki, S. Konishi, M. Ogata, *Nippon Juigaku. Zasshi* **40**, 375 (1978).
9. S. F. Cotmore and P. Tattersall, *Adv. Virus Res.* **33**, 91 (1987).
10. S. Kajigaya *et al.*, *Proc. Natl. Acad. Sci. U.S.A.* **88**, 4646 (1991).
11. K. E. Brown and B. J. Cohen, *J. Gen, Virol.* **73**, 2147 (1992).
12. J. T. Dodge, C. Mitchell, D. J. Hanahan, *Arch. Biochem. Biophys.* **110**, 119 (1963).
13. S. Shimomura *et al.*, *Blood* **79**, 18 (1992).
14. J. Folch, M. Lees, G. H. Sloane Stanley, *J. Biol. Chem.* **226**, 497 (1957).
15. H. G. Rose and M. Oklander, *J. Lipid Res.* **6**, 428 (1965).
16. W. W. Christie, *High-Performance Liquid Chromatography and Lipids* (Pergamon, Oxford, 1987).
17. D. M. Marcus, S. K. Kundu, A. Suzuki, *Semin. Hematol.* **18**, 63 (1981).
18. Purified glycoshingolipids (Sigma or BioCarb; 100 μl, 50 μg ml^{-1} methanol) were evaporated on a polystyrene microtiter plate, and nonspecific binding was blocked with 5% bovine albumin in

phosphate-buffered saline (overnight). We added B19 empty capsids (100 μl, 5 μg/ml) to each well (in quadruplicate) and detected binding by a mouse anti-B19 monoclonal antibody (Chemicon) followed by ^{125}I-labeled sheep anti-mouse antibody (Amersham). The radioactivity in each well was counted for 2 min with a γ counter. There was no specific binding with CDH or CTH (methanol alone, mean count of 241; CDH, mean count of 282; CTH, mean count of 244), and reduced binding to Forssman antigen (mean count of 2088) compared to globoside (mean count of 7458).

19. B19 capsids and mouse monoclonal antibody to globoside bound to the same band on Western blotting of red cell extract, perhaps to a putative "globoprotein" [Y. Tonegawa and S. Hakomori, *Biochem. Biophys. Res. Commun.* **76**, 9 (1977)]. However, this band was removed by digestion with lipase but not by proteases, more consistent with a glycolipid moiety.
20. P. P. Mortimer, R. K. Humphries, J. G. Moore, R. H. Purcell, N. S. Young, *Nature* **302**, 426 (1983).
21. A. E. von dem Borne *et al.*, *Br. J. Haematol.* **63**, 35 (1986).
22. In addition, our preliminary data indicate that individuals who lack P on their cells (blood-group p phenotype) have no evidence of previous infection with B19, compared with a B19 seroprevalence rate of 60% in the general population.
23. J. M. Liu, S. W. Green, T. Shimada, N. S. Young, *J. Virol.* **66**, 4686 (1992).
24. P. Rouger, P. Gane, C. Salmon, *Rev. Fr. Transfus. Immuno. Hematol.* **30**, 699 (1987).
25. S. J. Naides and C. P. Weiner, *Prenat. Diagn.* **9**, 105 (1989); A. L. Morey, J. W. Keeling, H. J. Porter, K. A. Fleming, *Br. J. Obstet. Gynaecol.* **99**, 566 (1992).
26. P. Levine, M. J. Celano, F. Falkowski, *Transfusion (Philadelphia)* **3**, 278 (1963).
27. C. E. Walsh *et al.*, *Proc. Natl. Acad. Sci. U.S.A.* **89**, 7257 (1992).
28. We thank A. von dem Borne and D. Marcus for anti-globoside antibody; M. Collett for the B19 capsids; J. Proctor for red cell typing; J. Storey and M. McCarthy for supply of the rare red cell types; and J. Moss, R. Blumenthal, and D. Roberts for helpful discussions.

2 March 1993; accepted 3 August 1993

In Vivo Gene Therapy of Hemophilia B: Sustained Partial Correction in Factor IX–Deficient Dogs

Mark A. Kay,* Steven Rothenberg, Charles N. Landen, Dwight A. Bellinger, Frances Leland, Carol Toman, Milton Finegold, Arthur R. Thompson, M. S. Read, Kenneth M. Brinkhous, Savio L. C. Woo†

The liver represents a model organ for gene therapy. A method has been developed for hepatic gene transfer in vivo by the direct infusion of recombinant retroviral vectors into the portal vasculature, which results in the persistent expression of exogenous genes. To determine if these technologies are applicable for the treatment of hemophilia B patients, preclinical efficacy studies were done in a hemophilia B dog model. When the canine factor IX complementary DNA was transduced directly into the hepatocytes of affected dogs in vivo, the animals constitutively expressed low levels of canine factor IX for more than 5 months. Persistent expression of the clotting factor resulted in reductions of whole blood clotting and partial thromboplastin times of the treated animals. Thus, long-term treatment of hemophilia B patients may be feasible by direct hepatic gene therapy in vivo.

Hemophilia B is an X-linked blood coagulation disorder resulting from a deficiency of factor IX production in the liver. The disease affects about 1 in 30,000 males and can result in severe bleeding episodes that require infusion of blood products that contain factor IX (*1*). As a result of previous human protein replacement therapy, about half of hemophilia B patients are infected with human immunodeficiency virus or hepatitis viruses. A virus-free and nonthrombogenic factor IX product is now available, but because of high costs the current treatment protocols do not include prophylaxis and therapy is initiated after bleeding begins. A number of tissues are target organs for somatic gene therapy of hemophilia B, including fibroblasts, myoblasts, endothelial cells, keratinocytes, and hepatocytes (*2*–*7*). Because the liver is the organ of factor IX synthesis, it represents a natural target for gene replacement therapy.

We have previously reported that hepatocytes can be transduced in vivo by infusion of recombinant retroviral vectors into the portal vasculature of mice after partial hepatectomy (*8*). To determine if the same can be achieved in larger animals (such as dogs), we infused an amphotropic retroviral vector (LBGpgk) that encodes the *Escherichia coli* β-galactosidase gene (*8*) directly into the portal vasculature of normal dogs three times 1 to 3 days after partial hepatectomy (Fig. 1). Two weeks later, hepatocytes were isolated and stained with 5-bromo-4-chloro-3-imdoyl-6-D-galactopyranoside (x-Gal) (Fig. 1A). Liver sections from these animals were similarly analyzed (Fig. 1B). The proportion of stained (blue) cells in Fig. 1 represents the in vivo transduction frequency of hepatocytes and was about 1 and 0.3% in two animals. Additional tissues, including kidney and spleen, did not stain blue with x-Gal. These transduction efficiencies are similar to that previously observed in mice (*8*). Routine histologic analysis revealed no pathologic conditions in the liver.

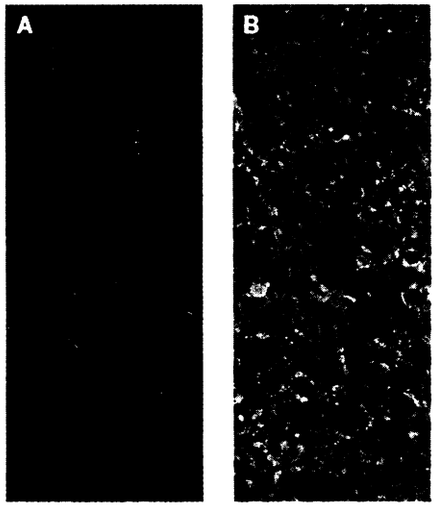

Fig. 1. Retroviral vector–mediated gene transfer of canine hepatocytes in vivo. A two-thirds partial hepatectomy was performed in two, 9-week-old normal dogs (3.5 kg) by resecting the left medial, left lateral, right medial, and caudate lobes. The right lateral lobe and its segmental blood supply and biliary drainage were preserved. The distal tip of a porta-cath catheter (Access Technology, Skokie, IL) was cannulated into a splenic vein. The injection port was placed subcutaneously under the right lateral abdominal wall. The LBGpgk vector was collected from confluent packaging cells cultured in Hg DMEM and 1% Hyclone for 12 hours. About 85 ml of filtered supernatants containing 9×10^7 colony-forming units was mixed with Polybrene (20 μg/ml) and infused over 45 to 90 min through the catheter 24, 48, and 72 hours after the hepatectomy. The animals tolerated the procedure well except for occasional vomiting and transient pallor during the beginning of the first infusion. When the dogs were killed, hepatocytes were isolated, cultured (*10*), and stained with x-Gal (*8*) (**A**) (original magnification, ×200), and (**B**) liver sections were stained with x-Gal and counterstained with neutral red (*8*) (original magnification, ×400).

M. A. Kay, Departments of Molecular Genetics and Cell Biology, Baylor College of Medicine, Houston, TX 77030.
S. Rothenberg, Department of Pediatric Surgery, Baylor College of Medicine, Houston, TX 77030.
C. N. Landen, D. A. Bellinger, M. S. Read, K. M. Brinkhous, Department of Pathology, University of North Carolina, Chapel Hill, NC 27599.
F. Leland, C. Toman, S. L. C. Woo, Howard Hughes Medical Institute, Department of Cell Biology, Baylor College of Medicine, Houston, TX 77030.
M. Finegold, Department of Pathology, Baylor College of Medicine, Houston, TX 77030.
A. R. Thompson, Puget Sound Blood Center, 921 Terry Avenue, Seattle, WA 98104.

*Present address: Markey Molecular Medicine Center, Department of Medicine RG-25, University of Washington, Seattle, WA 98195.
†To whom correspondence should be addressed.